Theoretical Temperature Dependence of the Mean-Square Displacements and Velocities of Surface Atoms of Face-Centered Cubic Crystals*

R. F. WALLIS
Naval Research Laboratory, Washington, D. C. 20390

AND

B. C. CLARK AND ROBERT HERMAN
Research Laboratories, General Motors Corporation, Warren, Michigan 48090

AND

D. C. GAZIS
IBM Watson Research Center, Yorktown Heights, N. Y. 10598

(Received 2 December 1968)

A theoretical investigation has been made of the temperature dependence of the mean-square displacements and velocities of surface atoms at a (110) free surface of a face-centered cubic crystal. A nearest-neighbor central-force model which provides a reasonable representation of nickel was used in the harmonic approximation. It was found that the mean-square displacements and velocities are essentially linear functions of temperature down to 200°K, or about one-half the bulk Debye temperature. Below 200°K, quantum-mechanical effects appear. Particular attention was paid to the temperature dependence of the anisotropy of the displacements and velocities associated with the (110) surface. Changes in the surface force constants were taken into acount.

I. INTRODUCTION

INFORMATION about the mean-square displacements and velocities of surface atoms of a crystal can be obtained from low-energy electron diffraction (LEED) studies and Mössbauer studies, respectively. In a previous paper[1] we have calculated the mean-square displacements of atoms on the (100), (110), and (111) surfaces of a fcc crystal in the high-temperature limit of the harmonic approximation and compared the results with MacRae's[2] LEED data on nickel. The theoretical calculations may be expected to be valid for temperatures well above the Debye temperature of the crystal. MacRae's data, however, extend down to temperature values quite close to the Debye temperature, so there is a question of the applicability of theoretical results based on the high-temperature approximation.

In the present paper we report a theoretical investigation of the temperature dependence of the mean-square displacements and velocities of surface atoms over a temperature range from 0°K to well above the Debye temperature. The calculations are made for a (110) surface of a fcc crystal using a nearest-neighbor central-force model in the harmonic approximation. The force-constants coupling-surface atoms to their neighbors have been permitted to deviate from the value for the coupling of wholly interior atoms, so that a reasonable fit to MacRae's nickel data[2] can be obtained.[3] It is found that the high-temperature approximation is valid to well below the bulk Debye temperature and that the anisotropies of the mean-square displacements and velocities at the surface are temperature-dependent at low temperatures.

II. THEORETICAL FORMULATION

We consider a fcc lattice with a pair of free surfaces normal to the [110] direction and with cyclic boundary conditions in the other two directions. We assume a nearest-neighbor central force model in which the force constants binding the surface atoms to their neighbors may be different from that characterizing the interactions of two interior atoms. The nearest-neighbor interactions of a surface atom for a (110) free surface can be classified into three different types. The interaction of type 1 couples the surface atom to an atom in an adjacent (110) plane, the line of centers of the two atoms making an angle of 30° with the surface. The type-2 interaction couples the surface atom with an atom two layers away and is normal to the surface. The type-3 interaction couples two atoms in the surface layer and is therefore parallel to the surface.

Associated with these interactions are three force constants α_1, α_2, and α_3, respectively, which need not be equal nor need they be equal to the force constant α characterizing the bulk material. A figure illustrating this situation is given in Ref. 3.

The equations of motion in the harmonic approximation have been given in detail in Ref. 3 and will not be repeated here. The temperature dependence of the ith

* Preliminary accounts of portions of this work were presented at the March 1968 meeting of the American Physical Society and at the Fourth International Materials Symposium held in Berkeley, Calif., June 19–21, 1968.

[1] B. C. Clark, R. Herman, and R. F. Wallis, Phys. Rev. **139**, A860 (1965).

[2] A. U. MacRae, in *International Conference on the Physics and Chemistry of Solid Surfaces, Brown University, 1964* (North-Holland Publishing Co., Amsterdam, 1964); Surface Sci. **2**, 522 (1964).

[3] R. F. Wallis, B. C. Clark, and R. Herman, Phys. Rev. **167**, 652 (1968).

components of the mean-square displacement and velocity of an atom labeled lmn is specified by the following expressions which are derived in the Appendix:

$$\langle u_{lmni}^2\rangle=(\hbar/2m_0N^2)\sum_{q_1,q_2}\left\{[D_c(q_1,q_2,+)]^{-1/2}\times\coth\frac{\hbar[D_c(q_1,q_2,+)]^{1/2}}{2kT}\right\}_{li,li},\quad(1)$$

$$\langle \dot{u}_{lmni}^2\rangle=\frac{\hbar}{2m_0N^2}\sum_{q_1,q_2}\left\{[D_c(q_1,q_2,+)]^{1/2}\times\coth\frac{\hbar[D_c(q_1,q_2,+)]^{1/2}}{2kT}\right\}_{li,li}.\quad(2)$$

In Eqs. (1) and (2), m_0 is the atomic mass, N is the number of atomic layers intercepting each edge of the parallelepiped, T is the absolute temperature, q_1 and q_2 are the components of the wave vector parallel to the surface, $D_c(q_1, q_2, +)$ is the reduced dynamical matrix defined in the Appendix, and the angular brackets denote an average over a canonical ensemble. For all sets of q_1,q_2 except (π,π) and $(2\pi,2\pi)$, Eqs. (1) and (2) were used in the calculations. For the sets (π,π) and $(2\pi,2\pi)$, which produce a zero eigenvalue of the reduced dynamical matrix, it was necessary to utilize the following alternative expressions, also derived in the Appendix, for the mean-square displacement and velocity components:

$$\langle u_{lmni}^2\rangle=(m_0N^2)^{-1}\sum_{q_1,q_2,p}[\xi_{cli}(q_1,q_2,p,+)]^2\times\frac{\bar{\epsilon}_c(q_1,q_2,p,+)}{[\omega_c(q_1,q_2,p,+)]^2},\quad(3)$$

$$\langle \dot{u}_{lmni}^2\rangle=(m_0N^2)^{-1}\sum_{q_1,q_2,p}[\xi_{cli}(q_1,q_2,p,+)]^2\times\bar{\epsilon}_c(q_1,q_2,p,+).\quad(4)$$

Here, $\omega_c(q_1, q_2, p, +)$ is the frequency of normal mode p, $\bar{\epsilon}_c(q_1, q_2, p, +)$ is the mean energy of the normal mode p, and $\xi_{cli}(q_1, q_2, p, +)$ is a component of the eigenvector of the reduced dynamical matrix.

In order to use Eqs. (1) and (2) in practical calculations, it is necessary to expand them in either the high-temperature or the low-temperature regime. The high-temperature expansions for the mean-square displacement and velocity components are

$$\langle u_{lmni}^2\rangle=\frac{kT}{m_0N^2}\sum_{q_1,q_2}\left\{[D_c(q_1,q_2,+)]^{-1}\times\sum_{n=0}^{\infty}\frac{2^{2n}}{(2n)!}B_{2n}\left(\frac{\hbar}{2kT}\right)^{2n}[D_c(q_1,q_2,+)]^n\right\}_{li,li},\quad(5)$$

$$\langle \dot{u}_{lmni}^2\rangle=\frac{kT}{m_0N^2}\sum_{q_1,q_2}\left\{\sum_{n=0}^{\infty}\frac{2^{2n}}{(2n)!}B_{2n}\times\left(\frac{\hbar}{2kT}\right)^{2n}[D_c(q_1,q_2,+)]^n\right\}_{li,li}.\quad(6)$$

In Eqs. (5) and (6) the quantities B_{2n} are the Bernoulli numbers as tabulated by Adams.[4] In the case of Eqs. (3) and (4) we only need the high-temperature limit expression for Eq. (3) which is

$$\langle u_{lmni}^2\rangle\approx\frac{kT}{m_0N^2}\sum_{q_1,q_2,p}[\xi_{cli}(q_1,q_2,p,+)]^2\times[\omega_c(q_1,q_2,p,+)]^{-2}.\quad(7)$$

At low temperatures the expansion of the hyperbolic cotangent in Eqs. (1) and (2) leads to a series of exponentials of matrices which are awkward for calculation. The 0°K terms, however, do not involve an exponential and have the form given as follows:

$$\langle u_{lmni}^2\rangle\approx\frac{\hbar}{2m_0N^2}\sum_{q_1,q_2}\{[D_c(q_1,q_2,+)]^{-1/2}\}_{li,li},\quad(8a)$$

$$\langle \dot{u}_{lmni}^2\rangle\approx\frac{\hbar}{2m_0N^2}\sum_{q_1,q_2}\{[D_c(q_1,q_2,+)]^{1/2}\}_{li,li}.\quad(8b)$$

The equations for $T=0$°K derived from Eqs. (3) and (4) are given by

$$\langle u_{lmni}^2\rangle\approx\frac{\hbar}{2m_0N^2}\sum_{q_1,q_2,p}[\xi_{cli}(q_1,q_2,p,+)]^2\times[\omega_c(q_1,q_2,p,+)]^{-1},\quad(9a)$$

$$\langle \dot{u}_{lmni}^2\rangle\approx\frac{\hbar}{2m_0N^2}\sum_{q_1,q_2,p}[\xi_{cli}(q_1,q_2,p,+)]^2\times\omega_c(q_1,q_2,p,+).\quad(9b)$$

III. RESULTS FOR NICKEL

We have carried out explicit calculations of the mean-square displacement and velocity components at a (110) surface using values of the force constants which give a reasonable fit to MacRae's LEED data for nickel,[2,3] namely, $\alpha_1=\frac{1}{2}\alpha$, $\alpha_2=\frac{1}{2}\alpha$, and $\alpha_3=\alpha$. The value of the bulk force constant α was determined by fitting the maximum frequency of the phonon dispersion curves[5] and is equal to 3.79×10^4 dyn/cm. It should be noted that this value of α gives a very good fit to the entire set of phonon dispersion curves.[1]

The calculations were carried out for finite crystals with one pair of free parallel surfaces and up to 20 atom

[4] E. P. Adams, *Smithsonian Mathematical Formulas* (Smithsonian Institution, Washington, D. C., 1947).

[5] R. J. Birgeneau, J. Cordes, G. Dolling, and A. D. B. Woods, Phys. Rev. 136, A1359 (1964).

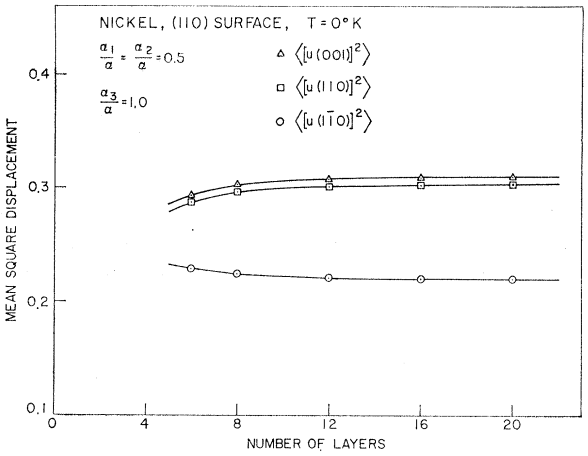

FIG. 1. The mean-square displacement components in units of 10^{-18} cm^2 plotted as a function of crystal thickness in atomic layers for $2\alpha_1 = 2\alpha_2 = \alpha_3 = \alpha$. The solid curves are visual fits to the calculated points.

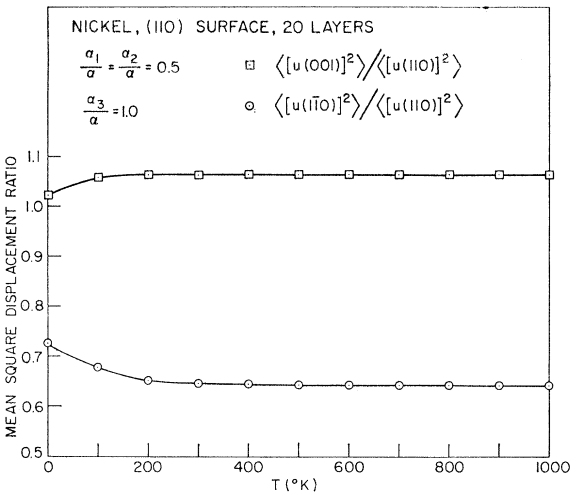

FIG. 3. The ratios of the parallel mean-square displacement components to the perpendicular component plotted as a function of absolute temperature for $2\alpha_1 = 2\alpha_2 = \alpha_3 = \alpha$. The solid curves are visual fits to the calculated points.

layers thick. Up to 20 terms were taken in the high-temperature expansions, although 10 terms were found to be sufficient in all the cases reported. The convergence of the series was quite good down to 90°K, about $\frac{1}{4}$ the bulk Debye temperature of nickel. We have found that at temperatures below 90°K, the inclusion of terms between the 10th and 20th did not yield satisfactorily convergent results.

The inverse matrices required in Eq. (5) were found numerically using the Gauss elimination method which yielded values of the diagonal elements accurate to six significant figures. The square roots of the matrices required in Eq. (8) were found using the Newton-Raphson method. For the sets of values of q_1, q_2 which yield zero eigenvalues of the dynamical matrix, Eqs. (7) and (9) were used with the eigenvalues and eigenvectors calculated by the method of Jacobi.[6] For all other sets of q_1, q_2, Eqs. (5), (6), and (8) were used.

Calculations were carried out to investigate the dependence of the surface mean-square displacement components on crystal thickness. The results for $T = 0$°K are shown in Fig. 1. Calculations were made for crystals having the numbers of atomic layers as indicated by the points shown. One notes for crystals twelve layers or more in thickness, that the surface mean-square displacement components remain essentially constant for

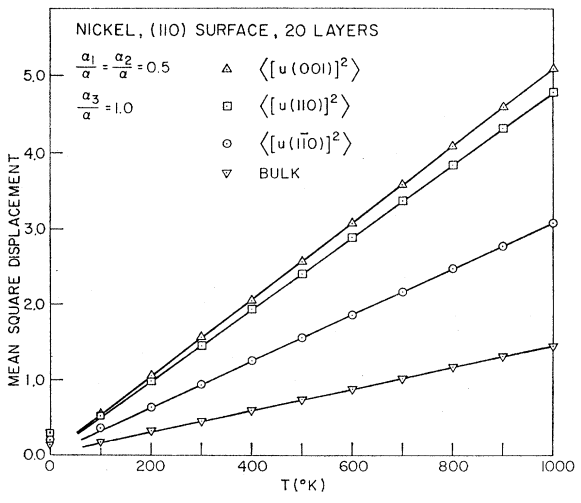

FIG. 2. The mean-square displacement components in units of 10^{-18} cm^2 plotted as a function of absolute temperature for $2\alpha_1 = 2\alpha_2 = \alpha_3 = \alpha$. The solid lines are visual fits to the high-temperature points.

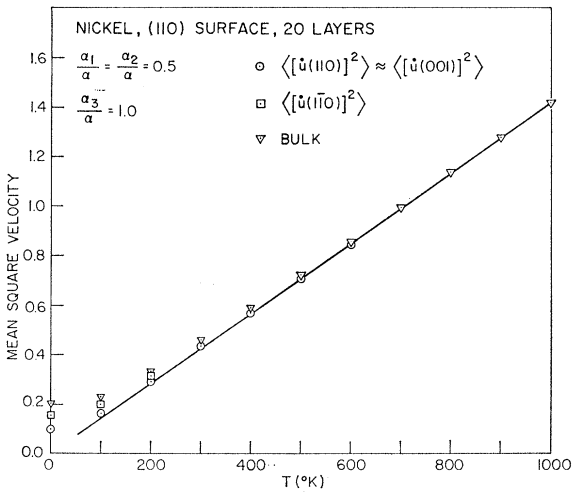

FIG. 4. The mean-square velocity components in units of 10^9 cm^2 sec^{-2} plotted as a function of absolute temperature for $2\alpha_1 = 2\alpha_2 = \alpha_3 = \alpha$. The solid line is a visual fit to the high-temperature points.

[6] J. H. Wilkinson, *The Algebraic Eigenvalue Problem* (Clarendon Press, Oxford, 1965).

each of the three directions. For the (110) free surface, the perpendicular and two parallel directions are all nonequivalent. For an atom well in the interior, however, the three directions are equivalent because of the cubic symmetry. The results given in Fig. 1 clearly show the anticipated anisotropy of the mean-square displacements at the surface. The qualitative behavior shown in Fig. 1 for the three components is also found at temperatures up to the high-temperature limit. When each of the surface force constants has the bulk value, it is interesting to note that the $(1\bar{1}0)$ mean-square displacement component increases with increasing crystal thickness, unlike the situation discussed above for $\alpha_3=2\alpha_1=2\alpha_2=\alpha$. The qualitative behavior $T=0°K$ presented here is also found at high temperatures.[1]

The temperature dependence of the mean-square displacement components for the case of 20 layers with $\alpha_3=2\alpha_1=2\alpha_2=\alpha$ is presented in Fig. 2. The points are computed values and the straight lines have been drawn through the high-temperature portions. One sees that the high-temperature linear behavior persists down below 200°K or $\frac{1}{2}$ the bulk Debye temperature, ~400°K. This result justifies the use of the high-temperature approximation in analyzing experimental data at room temperature and above.

In order to exhibit the behavior of the anisotropy in a clearer fashion we plot in Fig. 3, for the same case, the ratios of the parallel mean-square displacement components to the perpendicular component versus absolute temperature. The anisotropy is essentially constant down to temperatures of about 200°K and then decreases as the temperature decreases to 0°K.

The temperature dependence of the mean-square velocity components for the case of 20 layers with $\alpha_3=2\alpha_1=2\alpha_2=\alpha$ is shown in Fig. 4. Above room temperature all the mean-square velocity components, both surface and bulk, have essentially the classical value kT/m. Below room temperature the bulk value becomes larger than the surface values, all of which are decreasing less rapidly with temperature than the classical values. Furthermore, an anisotropy of the surface mean-square velocities appears at the lower temperatures. This anisotropy is exhibited more clearly in Fig. 5 where the ratios of the two parallel mean-square velocity components to the perpendicular component are plotted versus absolute temperature. The ratio $\langle[\dot{u}(001)]^2\rangle/\langle[\dot{u}(110)]^2\rangle$ is almost constant with temperature showing only a very slight decrease near 0°K, whereas the ratio $\langle[\dot{u}(1\bar{1}0)]^2\rangle/\langle[\dot{u}(110)]^2\rangle$ rises very rapidly below ~200°K and reaches a value ~50% larger than the former ratio at 0°K.

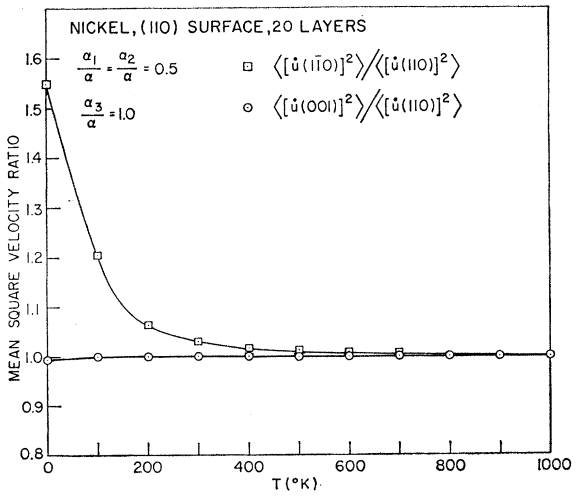

FIG. 5. The ratios of the parallel mean-square velocity components to the perpendicular component plotted is a function of absolute temperature for $2\alpha_1=2\alpha_2=\alpha_3=\alpha$. The solid curves are visual fits to the calculated points.

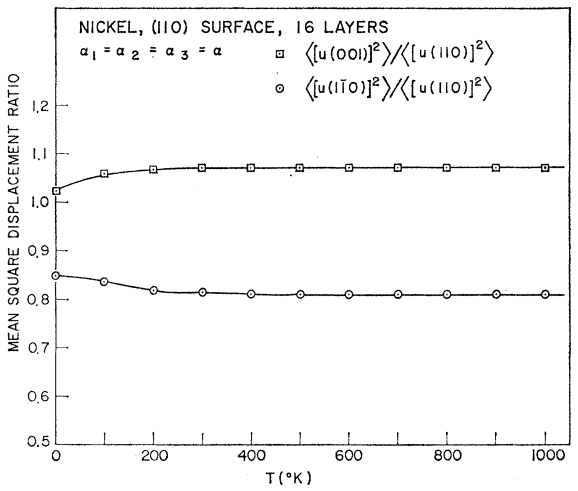

FIG. 6. The ratios of the parallel mean-square displacement components to the perpendicular component plotted as a function of absolute temperature for $\alpha_1=\alpha_2=\alpha_3=\alpha$. The solid curves are visual fits to the calculated points.

In addition to the calculations for the surface force constants chosen to give reasonably good agreement with the LEED experiments for nickel,[2] we have performed calculations with each of the surface force constants equal to the bulk value α. The results for the temperature dependence of the mean-square displacement component ratios are shown in Fig. 6. Comparing Figs. 3 and 6 one sees that the ratio $\langle[u(001)]^2\rangle/\langle[u(110)]^2\rangle$ has nearly the same temperature dependence in both cases. The qualitative behavior of the temperature dependence for the ratio $\langle[u(1\bar{1}0)]^2\rangle/\langle[u(110)]^2\rangle$ is similar in the two cases, but the curve for the unchanged force constant case is shifted to values about 25% higher than those for the changed force constant case.

The results for the temperature dependence of the mean-square velocity component ratios are shown in Fig. 7. As with the case of the changed force constants the ratio $\langle[\dot{u}(001)]^2\rangle/\langle[\dot{u}(110)]^2\rangle$ is essentially unity at all temperatures, and the ratio $\langle[\dot{u}(1\bar{1}0)]^2\rangle/\langle[\dot{u}(110)]^2\rangle$

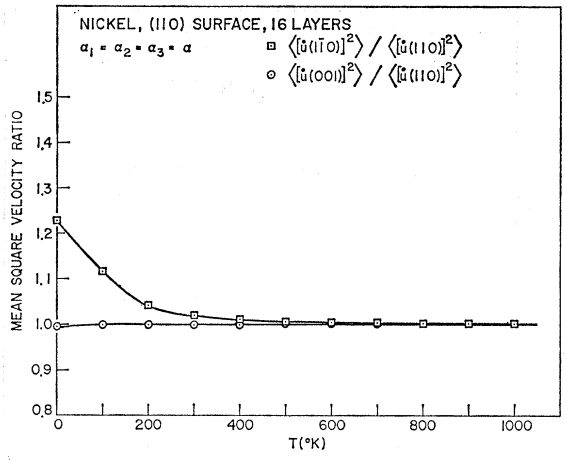

FIG. 7. The ratios of the parallel mean-square velocity components to the perpendicular component plotted as a function of absolute temperature for $\alpha_1=\alpha_2=\alpha_3=\alpha$. The solid curves are visual fits to the calculated points.

shows a rapid increase for temperatures below 200°K. The magnitude of the latter ratio, however, is significantly less at the lower temperatures than for the case of changed force constants.

IV. DISCUSSION

The results obtained in this paper indicate that the high-temperature approximation for the mean-square displacements can be applied for temperatures down to about $\frac{1}{2}$ the bulk Debye temperature of nickel. For surface atoms this approximation is quite good somewhat below the surface Debye temperatures determined by MacRae in Ref. 2, namely, 220°K for the [110] and [001] directions and 310°K for the [1$\bar{1}$0] direction.

It should be emphasized that we find the anisotropy of the mean-square displacements and velocities at a (110) free surface to be a consequence of the fundamental lack of symmetry at such a surface, and not to be intrinsically dependent upon changes in the surface force constants from their bulk value. Thus, all of the qualitative anisotropies are exhibited by our results for the case of unchanged surface force constants. However, the changes in the surface force constants do produce a significant effect on the magnitude of certain of the mean-square displacement and velocity ratios.

At all temperatures, the mean-square displacements and velocities reach very nearly their bulk values within five atomic layers of the surface. For the cases considered, the ratios of surface-to-bulk mean-square displacements are higher at high temperatures than at 0°K. The surface-to-bulk mean-square velocity ratios are significantly less than unity at 0°K and approach unity at high temperatures.

The changes in anisotropy at zero degrees compared to high temperatures appear to be sufficiently large to be experimentally observable. For mean-square displacements this could be accomplished by carrying out LEED measurements both at liquid-helium temperature and at higher temperatures. For mean-square velocities the corresponding experimental measurement would be that of second-order Doppler shifts of the Mössbauer effect.

Anharmonic effects have been completely neglected in the present paper. At temperatures well above the Debye temperature, one would expect anharmonic effects to become appreciable. Such effects would tend to increase the mean square displacements and decrease the mean square velocities, particularly at the surface.

ACKNOWLEDGMENT

It is a pleasure to acknowledge helpful discussions with Michael Marcotty, General Motors Research Laboratories, on certain aspects of the numerical calculations.

APPENDIX

Let u_{lmni} be the ith Cartesian component of displacement of an atom at the lattice site specified[8] by the integers l, m, and n. The crystal is taken to have the form of a rectangular parallelepiped with N atomic layers intercepting each of the three principal edges. The two free (110) surfaces correspond to $l=0$ and $l=N-1$. From the symmetry of the equations of motion[3] one is led to introduce the transformation

$$u_{lmni}(\pm)=\tfrac{1}{2}\sqrt{2}\,(u_{lmni}\pm u_{N-1-l,m,n,i}), \qquad \text{(A1)}$$

where now l is restricted to the range $0\leq l\leq(\frac{1}{2}N)-1$, and N is taken to be an even integer.

Introducing the wave-vector components q_1 and q_2 corresponding to cyclic boundary conditions in the y and z directions, we write the transformation to normal coordinates in the form

$$u_{lmni}(\pm)=(m_0N^2)^{-1/2}\sum_{\sigma=c,s}\sum_{q_1,q_2,p}T_\sigma(q_1,q_2)\times\xi_{\sigma li}(q_1,q_2,p,\pm)A_\sigma(q_1,q_2,p,\pm), \qquad \text{(A2)}$$

where

$$T_c(q_1,q_2)=\cos(mq_1+nq_2), \qquad \text{(A3a)}$$

$$T_s(q_1,q_2)=\sin(mq_1+nq_2), \qquad \text{(A3b)}$$

and the $A_\sigma(q_1, q_2, p, \pm)$ are the normal coordinates for mode p. The quantities $\xi_{\sigma li}(q_1, q_2, p, \pm)$, briefly, $\xi_{\sigma i}(\pm)$, are the components of the orthonormal eigenvectors of the dynamical matrix and can be grouped into the following sets of interacting variables: $[\xi_{c,1}(+), \xi_{s,2}(-), \xi_{s,3}(-)]$, $[\xi_{s,1}(+), \xi_{c,2}(-), \xi_{c,3}(-)]$, $[\xi_{c,1}(-), \xi_{s,2}(+), \xi_{s,3}(+)]$, and $[\xi_{s,1}(-), \xi_{c,2}(+), \xi_{c,3}(+)]$. These sets each contain $\frac{3}{2}N$ components and can be denoted by column vectors $\Psi_c(q_1, q_2, p, +)$, $\Psi_s(q_1, q_2, p, +)$, $\Psi_c(q_1, q_2, p, -)$, and $\Psi_s(q_1, q_2, p, -)$, respectively, which satisfy the equations

$$\omega_c^2(q_1, q_2, p, \pm)\Psi_c(q_1, q_2, p, \pm)=D_c(q_1, q_2, \pm)\Psi_c(q_1, q_2, p, \pm), \qquad \text{(A4a)}$$

$$\omega_s^2(q_1, q_2, p, \pm)\Psi_s(q_1, q_2, p, \pm)=D_s(q_1, q_2, \pm)\Psi_s(q_1, q_2, p, \pm), \qquad \text{(A4b)}$$

where $D_c(q_1, q_2, \pm)$, $D_s(q_1, q_2, \pm)$ are reduced dynamical matrices, and $\omega_c(q_1, q_2, p, \pm)$, $\omega_s(q_1, q_2, p, \pm)$ are the normal mode frequencies.

It will be seen below that only $D_c(q_1, q_2, \pm)$ is needed; explicit expressions for the model under consideration are given in the Appendix of Ref. 3.

From Eq. (A1) and the use of symmetry, one can write for the mean-square displacement components

$$\langle u_{lmni}{}^2\rangle=\tfrac{1}{2}\{\langle[u_{lmni}(+)]^2\rangle+\langle[u_{lmni}(-)]^2\rangle\}, \quad \text{(A5)}$$

where the angular brackets denote an average over a canonical ensemble. For $\langle[u_{lmni}(\pm)]^2\rangle$ we can write

$$\langle[u_{lmni}(\pm)]^2\rangle=(m_0N^2)^{-1}\sum_{\sigma=c,s}\sum_{q_1,q_2,p}[T_\sigma(q_1,q_2)]^2 \times[\xi_{\sigma li}(q_1, q_2, p, \pm)]^2\langle[A_\sigma(q_1, q_2, p, \pm)]^2\rangle, \quad \text{(A6)}$$

where we have used Eq. (A2) and the relation

$$\langle A_\sigma(q_1, q_2, p, \pm)A_\tau(q_1', q_2', p', \pm)\rangle =\langle[A_\sigma(q_1, q_2, p, \pm)]^2\rangle\delta_{q_1,q_1'}\delta_{q_2,q_2'}\delta_{p,p'}\delta_{\sigma,\tau}. \quad \text{(A7)}$$

In terms of the mean energy $\bar{\epsilon}_\sigma(q_1, q_2, p, \pm)$ we have

$$\langle[A_\sigma(q_1, q_2, p, \pm)]^2\rangle=\bar{\epsilon}_\sigma(q_1, q_2, p, \pm)/[\omega_\sigma(q_1, q_2, p, \pm)]^2, \quad \text{(A8)}$$

where

$$\bar{\epsilon}=(\hbar\omega/2)\coth(\hbar\omega/2kT), \quad \text{(A9)}$$

and the indices have been dropped from $\bar{\epsilon}$ and ω in Eq. (A9). Utilizing Eq. (A8) and a theorem of matrices[7] we can carry out the sum over p in Eq. (A6) to yield

$$\langle[u_{lmni}(\pm)]^2\rangle=\frac{\hbar}{2m_0N^2}\sum_\sigma\sum_{q_1,q_2}[T_\sigma(q_1,q_2)]^2 \times\left\{[D_\sigma(q_1, q_2, \pm)]^{-\frac{1}{2}}\coth\frac{\hbar[D_\sigma(q_1, q_2, \pm)]^{1/2}}{2kT}\right\}_{li,li}. \quad \text{(A10)}$$

[7] M. Born, Rept. Progr. Phys. 9, 294 (1942).

From the forms of the reduced dynamical matrices it is clear that

$$D_c(\pi+q_1, \pi+q_2, \pm)=D_s(\pi-q_1, \pi-q_2, \pm). \quad \text{(A11)}$$

Using Eq. (A11) and the properties of the trigonometric functions we obtain

$$\langle[u_{lmni}(\pm)]^2\rangle=\frac{\hbar}{2m_0N^2}\sum_{q_1,q_2}\left\{[D_c(q_1, q_2, \pm)]^{-1/2} \times\coth\frac{\hbar[D_c(q_1, q_2, \pm)]^{1/2}}{2kT}\right\}_{li,li}. \quad \text{(A12)}$$

For all cases of interest, one finds that the contributions of $+$ and $-$ in Eq. (A12) are equal; hence, using Eq. (A5), we get

$$\langle u_{lmni}{}^2\rangle=\frac{\hbar}{2m_0N^2}\sum_{q_1,q_2}\left\{[D_c(q_1, q_2, +)]^{-1/2} \times\coth\frac{\hbar[D_c(q_1, q_2, +)]^{1/2}}{2kT}\right\}_{li,li}. \quad \text{(A13)}$$

Again using the theorem of matrices referred to above, we transform Eq. (A13) to the form

$$\langle u_{lmni}{}^2\rangle=(m_0N^2)^{-1}\sum_{q_1,q_2,p}[\xi_{cli}(q_1, q_2, p, +)]^2 \times\frac{\bar{\epsilon}_c(q_1, q_2, p, +)}{[\omega_c(q_1, q_2, p, +)]^2}. \quad \text{(A14)}$$

For the mean-square velocity components, the essential point to note is that the time derivative of the normal coordinate A is proportional to the corresponding normal mode frequency times A. The expression for the mean square velocity component analogous to Eq. (A6) then contains an extra factor of the normal mode frequency squared. The remainder of the derivation follows the lines already indicated.